

## Development and characterization of starch nanoparticles by gamma radiation: Potential application as starch matrix filler

Melisa Lamanna<sup>a</sup>, Noé J. Morales<sup>b</sup>, Nancy Lis García<sup>a,c</sup>, Silvia Goyanes<sup>a,\*</sup>

<sup>a</sup> LPMC, Departamento de Física, Facultad de Ciencias Exactas y Naturales and IFIBA (CONICET), Universidad de Buenos Aires, Ciudad Universitaria, 1428, Ciudad Autónoma de Buenos Aires, Argentina<sup>1</sup>

<sup>b</sup> INQUIMAE, CONICET-UBA, Ciudad Universitaria, Pab2, C1428EHA, Bs As, Argentina

<sup>c</sup> CIHIDECAR-CONICET, Dpto. de Química Orgánica, Facultad de Ciencias Exactas y Naturales, Universidad de Buenos Aires, Ciudad de Buenos Aires, 1428, Buenos Aires, Argentina

### ARTICLE INFO

#### Article history:

Received 30 January 2013

Received in revised form 19 April 2013

Accepted 20 April 2013

Available online 3 May 2013

#### Keywords:

Starch nanoparticles

Gamma radiation

Starch composite

### ABSTRACT

Gamma radiation arises as an advantageous alternative to obtain starch nanoparticles given its low cost, simple methodology and scalability. Starch nanoparticles (SNP) with sizes around 20 and 30 nm were obtained applying a dose of 20 kGy from cassava (CNP- $\gamma$ ) and waxy maize (WNP- $\gamma$ ) starch, respectively. They showed the same thermal degradation behavior and their maximum mass loss zone was similar to those nanoparticles obtained from acid hydrolysis (WNP-h). Additionally, CNP- $\gamma$  and WNP- $\gamma$  were used as nanofillers in a cassava matrix. Increments of 102% in storage modulus were obtained with the addition of only 2.5 wt.% of WNP- $\gamma$ , showing that gamma radiation is a successful methodology to obtain SNP able to be used as starch reinforcement.

© 2013 Elsevier Ltd. All rights reserved.

## 1. Introduction

Starch has received considerable attention during the past decades as a biodegradable thermoplastic polymer and as biodegradable particulate filler. The main advantages of starch fillers are: their renewable nature; availability; high specific strength; non-abrasive nature that allows easier processing even at high filling levels; biodegradability; and a relatively reactive surface which can be modified by adding reactive groups compatible with the polymeric matrix (García et al., 2012; Le Corre, Bras, & Dufresne, 2010). It is well known that it is possible to obtain starch nanoparticles (SNP) by starch acid hydrolysis (García, Ribba, Dufresne, Aranguren, & Goyanes, 2009). These nanoparticles were used to reinforce different kinds of matrices, such as starch (García, Ribba, Dufresne, Aranguren, & Goyanes, 2011), PVA (Sreekumar, Al-Harthi, & De, 2012), and synthetic latex (Dufresne & Cavaille, 1998). As a consequence of the particle nanometric size, their addition in very small amounts produces significant improvements in the mechanical and permeation properties of different matrices (Duquesne, Habibi, & Dufresne, 2012; García et al., 2011; Labet, Thielemans, & Dufresne, 2007; Piyada, Waranyou, & Thawien, 2013). In particular, the incorporation of SNP in starch matrices led to improvements in

elastic modulus and water vapor resistance (Behera, Avancha, Sen, & Adhikari, 2013; García et al., 2009).

Starch consists of mainly two glucosidic macromolecules: amylose and amylopectin. According to Jenkins et al. (1994), the crystallinity of starch granule is associated with the amylopectin component. Besides, the authors proposed a model considering the shells to be formed by alternating crystalline–amorphous layers. It is noteworthy that the amylopectin content depends on the botanic origin.

Gamma radiation ( $\gamma$ -radiation) can be a convenient tool for modification of polymer materials through cross-linking, grafting and degradation techniques. It has also been suggested as a rapid and convenient modification technique which breaks large molecules into smaller fragments and is capable of cleaving glucosidic linkages (Singh, Singh, Ezekiel, & Kaur, 2011). Gamma radiation may generate free radicals on starch molecules which are capable of hydrolyzing chemical bonds, thereby cleaving large molecules of starch into smaller fragments of dextrin (Yu & Wang, 2007). In particular, it is expected that  $\alpha$ -D-(1-4)-glycoside linkages are the most susceptible bonds to be cleaved by  $\gamma$ -radiation. Bao, Ao, and Jane (2005) investigated how gamma radiation affects the structures and physical properties of starch in order to understand the mechanisms which affect starch granule structures. They concluded that fragmentation mostly resulted from the cleavage at the amorphous regions, instead of crystallite regions, but little changes in the amylopectin branch chain length occurred. This mechanism was similar to that of the starch acid hydrolysis (Bank,

\* Corresponding author. Tel.: +54 11 45763300x255; fax: +54 11 45763357.

E-mail address: [goyanes@df.uba.ar](mailto:goyanes@df.uba.ar) (S. Goyanes).

<sup>1</sup> <http://www.lpmc.df.uba.ar>.

Greenwood, & Muir, 1973; Hoover, 2000). It is important to mention that although free radicals could be involved in the mechanism they easily recombine in water, thus solutions obtained from gamma irradiated samples are radical free.

Akhavan and Ataevarjovi (2012) have recently showed that gamma radiation would be an effective protocol in the size reduction of particles based on soluble starch. The mean size of these particles could be changed by the use of surfactants during the formation process under gamma irradiation. On the contrary,  $\gamma$ -irradiated solid starch samples have produced different results, as reported by Singh et al. (2011). In that research, it was observed that the intensity of XRD peaks decreased by increasing the irradiation dose for potato starch from two different cultivars. They employed gamma radiation from 0.01 to 0.5 kGy and concluded that starch irradiated at 0.5 kGy did not show presence of any organized crystalline structure. However, Bao et al. (2005) studied physical and structural characteristics of rice flour and starch obtained from gamma irradiated white rice at different doses between 0.5 and 9.0 kGy. These authors showed that the crystallinity increased in irradiated starch. The shape and size of starch particles depend strongly on its botanic origin. Then, the kind of native starch and the processing technique determine the starch properties after irradiation process.

The aim of this work is to develop starch nanoparticles applying gamma radiation, since this technique is commonly employed for food industries and would allow the SNP mass production with low costs. The influence of amylopectin content in the morphology, structure and thermal response was studied employing two different kinds of starch: native cassava and native waxy maize. The gamma radiation was carried out in both starch water dispersions. In order to compare the properties of SNP from waxy maize starch obtained by this novel procedure with one of the traditional methods, acid hydrolysis was also carried out.

Finally, the possibility of using the nanoparticles that have been obtained applying gamma radiation as starch matrix nanofiller was also studied.

## 2. Experimental

### 2.1. Materials

The native cassava starch (CS) (72 wt.% amylopectin and 28 wt.% amylose) was provided by Bernesa S.A., Buenos Aires, Argentina. The native waxy maize starch (WS) (99 wt.% amylopectin) was provided by Roquette S.A., Lestrem, France. The starches are native. None of these starches have received any physical or chemical modification. It was provided as supplementary data scanning electron micrographs for both starch types. The average size of cassava starch granule was 10  $\mu\text{m}$  with a standard dispersion of  $\sigma = 3 \mu\text{m}$ . In the case of waxy maize starch granule the average size was 11  $\mu\text{m}$  with a standard dispersion of  $\sigma = 4 \mu\text{m}$ .

### 2.2. Starch nanoparticles obtained by acid hydrolysis

In order to compare nanoparticles obtained by gamma radiation with the ones obtained by the traditional methodology, waxy maize nanoparticles were obtained by acid hydrolysis as previously reported (García et al., 2009). We employed 36.725 g of waxy maize starch and then mixed in 250 mL of  $3.16 \times 10^{-3} \text{ M H}_2\text{SO}_4$ , at 40 °C and 100 rpm, subjected to an orbital shaking action for 5 days. After that, crystals were washed in distilled water and separated by successive centrifugations until neutrality was reached. They were lyophilized and the powders obtained were named WNP-h.

### 2.3. Starch nanoparticles obtained by gamma irradiation

In order to prepare the samples to be treated by gamma radiation, starch stable dispersions were prepared according to the well known process (Vogel, 1983, chap. IX): 5 g of starch were mixed with 5 mL of distilled water at room temperature using a mechanic stirring at 180 rpm obtaining an homogenous paste. After that, this paste was quantitatively transferred to a 500 mL glass beaker. Then 495 mL of distilled water at 85 °C were added with magnetic stirring for 30 s. Immediately, the beaker was cooled at 5 °C and stored at room temperature in a hermetic vessel. This procedure let us to achieve cassava and waxy stable dispersions (CSD and WSD) for at least 1 month, without employing any other additives.

After obtaining these stable dispersions, samples were irradiated with 20 kGy using  $^{60}\text{Co}$  gamma-ray source facility of the Ezeiza Atomic Center-Argentina. The irradiation was developed at room temperature with an irradiation rate of 14 kGy/h. Both irradiated and non-irradiated samples were lyophilized. The obtained powders for the non irradiated stable dispersions were named CPD (cassava powders from stable dispersion) and WPD (waxy powders from stable dispersion). On the other hand, the powders obtained after gamma irradiation and lyophilization were named CNP- $\gamma$  and WNP- $\gamma$  for cassava and waxy starch, respectively.

### 2.4. Preparation of plasticized starch films

Thermoplastic starch was processed by casting as previously reported (García et al., 2009) from the mixing of native cassava-starch granules, glycerol and distilled water. A quantity of 15 g of a starch/glycerol mixture (3:1 by weight) was dispersed in 179 g of distilled water. The mixture was heated from room temperature at a heating rate of 1.59 °C/min under magnetic stirring for 28 min until gelatinization, which occurred at 70 °C. After gelatinization, the gel was degassed for 10 min with a vacuum mechanical pump. At that point, the composite films were prepared by adding the suspension of both starch nanoparticles (CNP- $\gamma$  and WNP- $\gamma$ ) in the desired quantities (2.5 wt.% relative to the total mass). After that, the mixture was stirred for 10 min at 250 rpm and degassed for another 5 min. Then, the mixture was cast in a plastic mould and evaporated in a ventilated oven at 50 °C for 48 h. Solid films having a thickness between 300 and 400  $\mu\text{m}$  were obtained. Matrix and composite films were stored at 43% relative humidity (RH) ( $\text{K}_2\text{CO}_3$  saturated solution) for 2 weeks before characterization. In order to study the modifications due to the incorporation of starch nanoparticles, matrix films were also developed by using the same methodology.

## 2.5. Characterization

### 2.5.1. Field emission scanning electron microscopy (FE-SEM)

Field emission scanning electron microscopy (FE-SEM) was performed using a Zeiss DSM982 Gemini with a field emission gun (FEG), to examine the morphology of starch nanoparticles. All the samples were observed with an acceleration voltage of 5 kV.

Samples obtained after gamma irradiation were observed using two different sample deposition methodologies. For the first one we employed dispersions in deionized water of lyophilized samples (CNP- $\gamma$  and WNP- $\gamma$ ). Drops of these dispersions were put onto silicon waffer and dried in vacuum during 24 h. For the second methodology, lyophilized samples were sprinkled onto a carbon tape. The same processes were employed to study nanoparticles obtained by acid hydrolysis methodology (WNP-h).

Cryogenic fracture surfaces of plasticized starch films (matrix and matrix with each SNP) were observed using field emission scanning electron microscopy (FE-SEM).

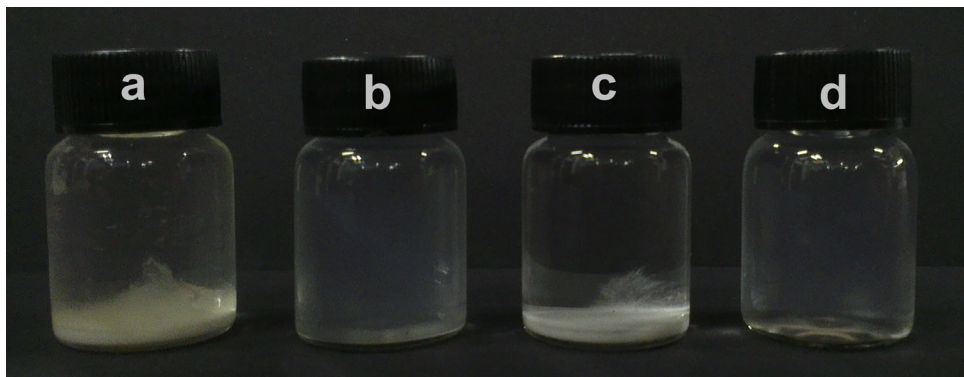


**Fig. 1.** Starch suspensions of (a) native waxy maize, (b) waxy maize stable dispersion (WSD) at 10 mg/mL, (c) waxy maize stable dispersion (WSD) at 15 mg/mL after 15 min of its preparation, and (d) waxy maize irradiated dispersion (WNP- $\gamma$ ) at 15 mg/mL after days of its preparation.

#### 2.5.2. Transmission electron microscopy (TEM)

Transmission electron microscopy (TEM) was performed with an EM 301 Philips transmission electron microscope at an acceleration voltage of 60 kV. Samples were prepared from diluted suspensions of CNP- $\gamma$  and WNP- $\gamma$  in deionized water. A drop of each sample was deposited onto a carbon coated microscopy grid and negatively stained with an aqueous 2% solution of uranyl acetate for 1 min. The liquid in excess was blotted with filter paper and the remaining liquid was dried before the specimen observation.

#### 2.5.3. Dynamic light scattering

Dynamic light scattering was performed employing a 90Plus/BIMAS Multi Angle Particle Sizing Option (Brookhaven Instruments Corporation). The samples analyzed were native starches (CS and WS) and irradiated samples (CNP- $\gamma$  and WNP- $\gamma$ ). Deionized water starch dispersions with concentration of 0.01 mg/mL were prepared using a tip sonicator during 20 min. Immediately, DLS measurements were done in order to avoid sample precipitation.

#### 2.5.4. X-ray diffraction (XRD)

The X-ray diffraction (XRD) analysis was conducted with a Siemens D 5000 X-ray diffractometer. The X-ray generator tension and current were 40 kV and 30 mA, respectively. The radiation was Cu K $\alpha$  of wavelength 1.54 Å. Data were collected from  $2\theta$  of 6.00° to 32.00° ( $\theta$  being the angle of diffraction) with a 0.02° step size.

The powders analyzed were the native starch (CS and WS), lyophilized stable dispersion before irradiation (CPD and WPD) and irradiated samples (CNP- $\gamma$  and WNP- $\gamma$ ). Nanocrystals obtained by hydrolysis methodology (WNP-h) were also analyzed.

#### 2.5.5. Thermal characterization

Samples for thermal characterization (WNP-h, CS, WS, CPD, WPD, CNP- $\gamma$  and WNP- $\gamma$ ) were previously stored at 33% relative humidity (MgCl<sub>2</sub> saturated solution) during 5 days. This characterization was carried out in a simultaneous TGA-DTA DTG-60 Shimadzu. The samples were heated from room temperature to 220 °C at 5 °C/min with nitrogen flux of 30 mL/min.

#### 2.5.6. Dynamic mechanical tests

Dynamic mechanical measurements were performed for the cassava starch matrix film and the composites with CNP- $\gamma$  and WNP- $\gamma$ , using a dynamic mechanical thermal analyzer (DMTA IV, Rheometric Scientific) in the rectangular tension mode at 1 Hz, in the temperature range -90 to 70 °C at a heating rate of 2 °C/min. Samples were subjected to a cyclic strain lower than 0.04% assuring that the mechanical response within the linear viscoelastic range. The set up was used to determine the storage modulus.

### 3. Results and discussion

The dispersion of native starches granules, CS and WS (1 mg/mL) precipitated after 15 min of its preparation. In Fig. 1a it can be seen waxy maize dispersion as an example. CS and WSD at 10 mg/mL remain stables for at least 1 month (Fig. 1b). However, at higher concentration (15 mg/mL), they precipitated after 15 min (Fig. 1c). Meanwhile, dispersion of irradiated samples (CNP- $\gamma$  and WNP- $\gamma$ ) remained stable even at a concentration as high as 15 mg/mL (Fig. 1d), suggesting that  $\gamma$ -radiation produce nanoparticles. If the particles are small enough in mass and size, they are subjected to Brownian motion and can form a stable and homogeneous dispersion. (Jolivet, Livage, & Henry, 2000).

#### 3.1. Morphological characterization

FE-SEM micrographs of nanoparticles obtained applying  $\gamma$ -radiation (CNP- $\gamma$  and WNP- $\gamma$ ) are shown in Fig. 2(a-d). It is possible to see particles with diameter below 100 nm. It should be noted that all samples were prepared with deionized water in order to avoid salts crystals to be present as impurities. In micrographs it is possible to observe nanoparticles with diameters around 30 nm or less, but aggregates of 100 nm were also observed. Nanoparticles tended to cluster together; this effect was clearly observed if micrographs of powders were observed. Therefore, FE-SEM micrographs were obtained for WNP- $\gamma$  and CNP- $\gamma$  powders sprinkled onto carbon type (Fig. 2e and f). In both cases, it can be observed the formation of laminar aggregates with large specific area. Similar structures were observed for WNP-h (not shown) and previously reported (García et al., 2009) for waxy maize nanocrystals obtained by acid hydrolysis. Additionally, as they reported, the existence of nanocrystals aggregates suggests the presence of a high number of OH-groups per individual nanocrystal, which becomes strongly associated by hydrogen bonding.

TEM micrograph of CNP- $\gamma$  and WNP- $\gamma$  are shown in Fig. 3. For waxy maize irradiated sample (Fig. 3a) it was possible to observe nanoparticles that have an average size below 40 nm. It must be noted that many small nanoparticles (below 30 nm) could be observed (blue circle). In the case of cassava irradiated sample (Fig. 3b), small nanoparticles with an average size of 20 nm were observed, but these ones form aggregates (red circle) with an average size higher than 50 nm. In particular, for CNP- $\gamma$  not only nanoparticles were observed but also some nanowires were present.

In order to study the size distribution of the nanoparticles obtained, we performed DLS analysis. The histogram obtained for CNP- $\gamma$  and WNP- $\gamma$  is shown in Fig. 4. As can be seen, the distribution for CNP- $\gamma$  was smaller than the one obtained for WNP- $\gamma$ .

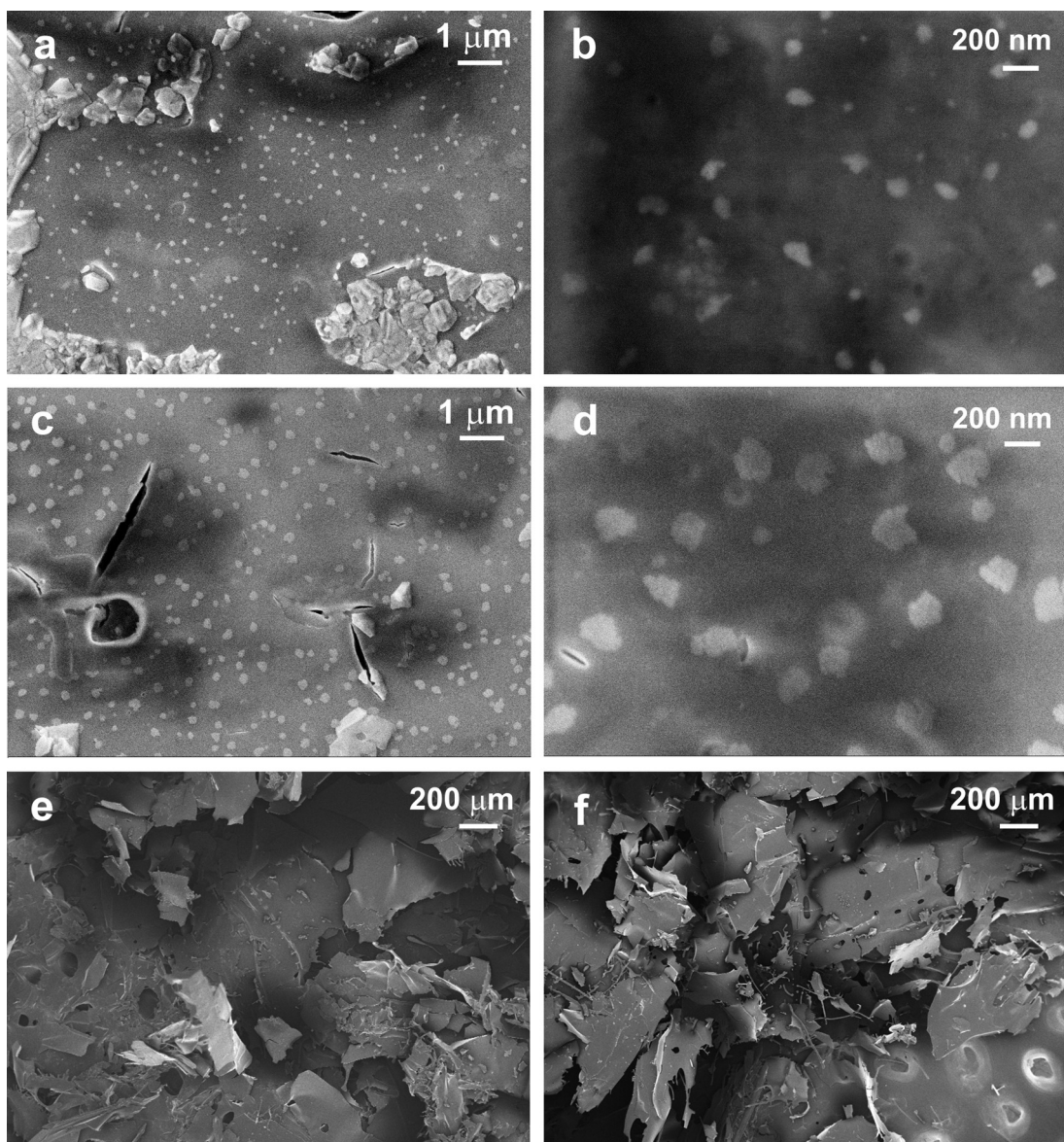


**Fig. 2.** FE-SEM micrographs for drops of WNP- $\gamma$  (a) and (b); CNP- $\gamma$  (c) and (d). Micrographs for sprinkled samples of WNP- $\gamma$  (e) and CNP- $\gamma$  (f).

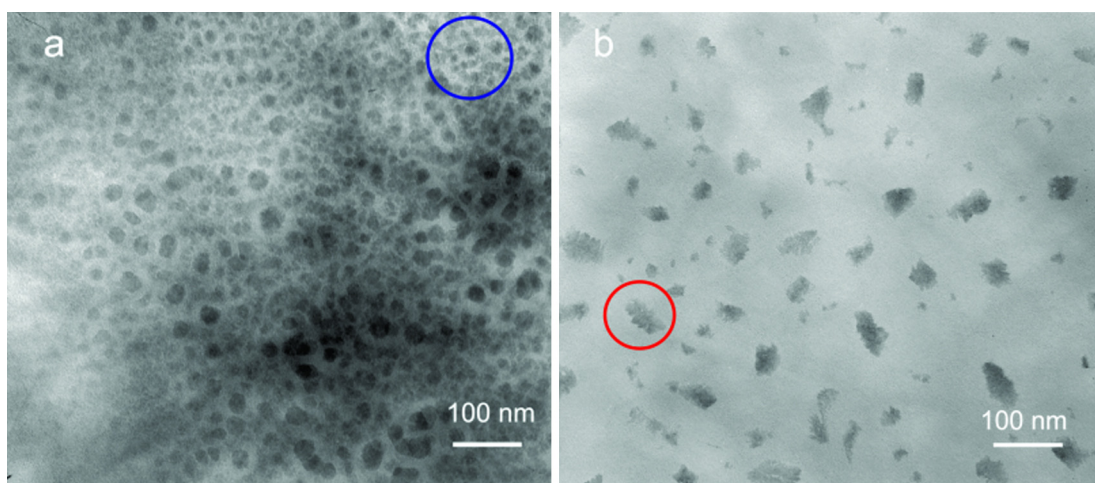


**Fig. 3.** TEM images for (a) waxy maize irradiated starch (WNP- $\gamma$ ), (b) cassava irradiated starch (CNP- $\gamma$ ).

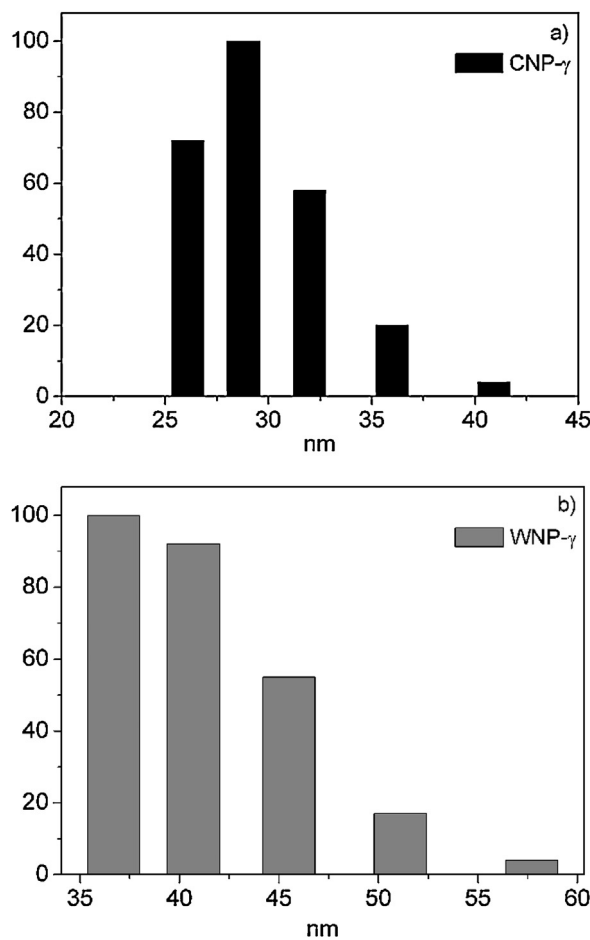


Fig. 4. DLS histograms obtained for (a) CNP- $\gamma$  (black) and (b) WNP- $\gamma$  (grey).

The most probable diameter for CNP- $\gamma$  is  $(29 \pm 5)$  nm and its average diameter was  $(31 \pm 5)$  nm, while for WNP- $\gamma$  the most probable diameter is  $(37 \pm 7)$  nm and its average diameter was  $(41 \pm 7)$  nm. It must be mentioned that DLS analysis provides the nanoparticle hydrodynamic radius.

Native starches contain between 15% and 45% of crystalline depending on the botanic origin (Le Corre et al., 2010). XRD patterns for nanoparticles obtained by  $\gamma$ -radiation and acid hydrolysis are shown in Fig. 5a. WNP-h showed a typical A type pattern with a  $(53 \pm 3)\%$  of crystallinity in agreement with Angellier, Molina-Bousseau, Dole, and Dufresne (2006), meanwhile CNP- $\gamma$  and WNP- $\gamma$  had an amorphous pattern. To explore if gamma radiation had produced any modification in the sample crystallinity, a comparison between XRD patterns before and after irradiation were performed (Fig. 5b). Furthermore, the XRD patterns of initial starches were also included.

The crystalline structures of the native starches (CS and WS) showed the typical patterns for both starch types (Angellier et al., 2006; Pimentel et al., 2007). However, amorphous patterns were observed for lyophilized powders obtained from starch stable dispersion before irradiation (CPD and WPD), suggesting that the treatment carried out, previously to irradiation process, produced the complete gelatinization of starch.

After gamma radiation, the CNP- $\gamma$  and WNP- $\gamma$  diffraction patterns seem to show two wide peaks with low intensity at  $2\theta = 6.5^\circ$  and  $2\theta = 12.5^\circ$ . Wide peaks in a XRD pattern suggest the presence of nanometric crystalline particles or amorphous material (Solinas, Piccaluga, Morales, & Serna, 2001). In any of the two cases, the

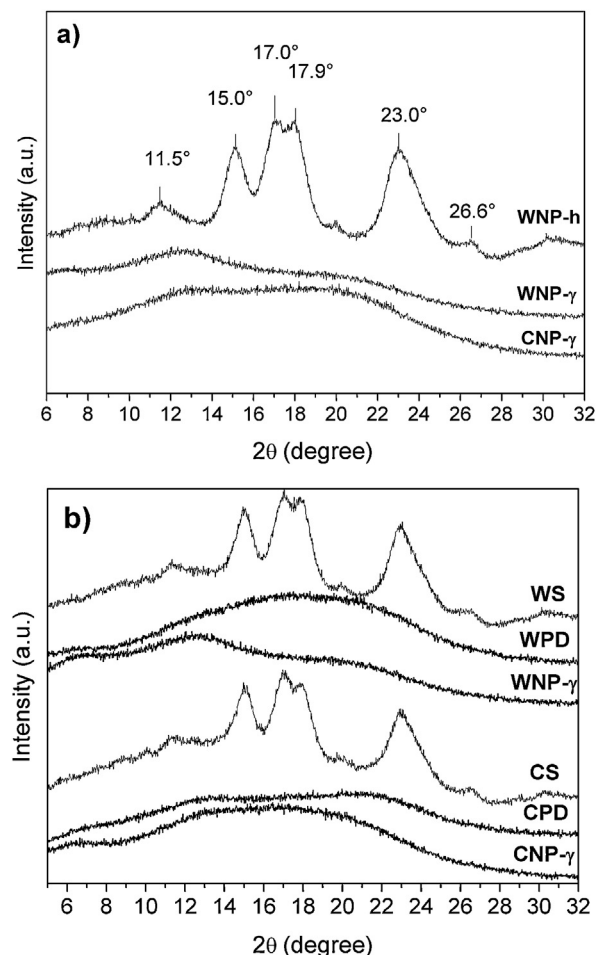


Fig. 5. (a) XRD pattern for nanoparticles obtained by hydrolysis (WNP-h) and gamma radiation (WNP- $\gamma$  and CNP- $\gamma$ ). (b) XRD pattern for lyophilized starch stable dispersions (WPD and CPD) and irradiated samples (WNP- $\gamma$  and CNP- $\gamma$ ).

amorphous component in samples (CNP- $\gamma$  and WNP- $\gamma$ ) is bigger than the crystalline one (Fig. 5b).

### 3.2. Thermal characterization

In Fig. 6a and b the degradation curves for all samples obtained from waxy maize and cassava starch, respectively are shown. It must be noted that regardless of the starch botanic source, the powders obtained from the stable dispersions before irradiation, degraded at lower temperature than native starches and their weight loss occurred abruptly with a slope similar to CS and WS.

Nanoparticles obtained by  $\gamma$ -radiation, for both starch types, showed the same thermal degradation behavior and their maximum weight loss zone was similar to those starch nanoparticles obtained from acid hydrolysis.

Also, it could be observed that irradiated samples (CNP- $\gamma$  and WNP- $\gamma$ ) began to lose weight at a temperature lower than the native starches (CS and WS) and the powders from stable suspensions (CPD and WPD), in agreement with what was observed for other irradiated polysaccharides (Xu, Sun, Yang, Ding, & Pang, 2007). This fact suggests that starch nanoparticles have a high number of hydroxyl groups on their surface and it is through them that the thermal degradation start, similar to what was already reported for starch nanoparticles obtained by acid hydrolysis (García et al., 2012). Furthermore, regardless of the obtaining process (irradiation or hydrolysis) nanoparticles presented a weight loss at a broad temperature range as a consequence of the sample

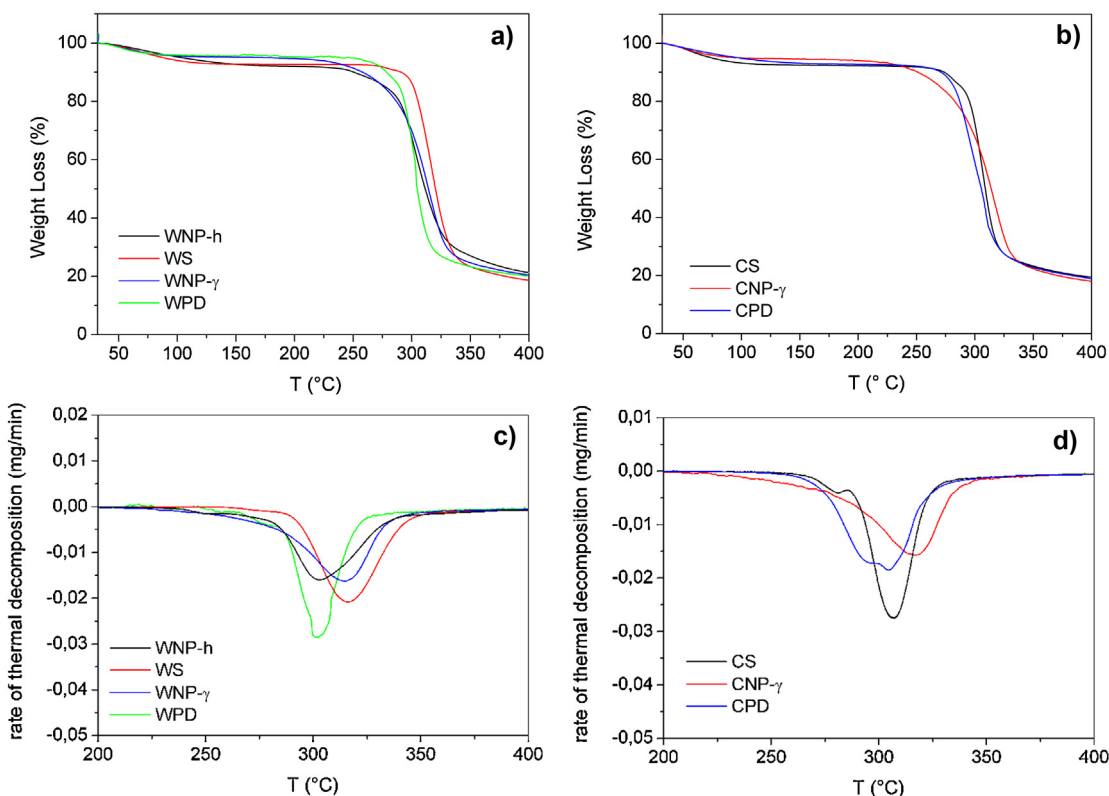


**Fig. 6.** TG analysis for (a) waxy maize and (b) cassava samples. Rate of thermal decomposition for (c) waxy and (d) cassava samples.

heterogeneity. This result could be due to a greater dispersion of molecular weights generated by gamma radiation (Guven, 2009) or hydrolysis treatment (Angellier-Coussy et al., 2009). The fact that the temperature range was broadened can be clearly seen from curves of thermal decomposition rate (Fig. 6c and d) as was described by many authors (Eid, Abdel-Ghaffar, & Dessouki, 2009; El-Arnaouty, Eid, Salah, & Hegazy, 2012).

In Fig. 7 the results of DTA analysis are shown. Gelatinization peak was observed around 70 °C for WS and about 55 °C for CS. In the case of WNP-h, the gelatinization peak observed at 70 °C is due to (47 ± 3%) of the amorphous component as was seen by XRD analysis. It must be mentioned that acid hydrolysis was carried out at 40 °C hence the amorphous component did not gelatinized. This endotherm peak is not related with crystalline component fusion, which is observed at higher temperatures. According to Garcia, Colonna, Bouchet, and Gallant (1997), for native cassava starch with water content between 20% and 60% DSC thermograms showed two endothermic peaks. The first peak is due to the gelatinization process, associated with further loss of starch crystallinity. Meanwhile, the second one is related to the remaining crystallites fusion.

Although native starch samples showed the gelatinization peak, for CNP-γ, WNP-γ, and for CPD and WPD it was absent. This fact could be explained taking into account that the treatment employed to prepare stable suspensions probably caused starch gelatinization. Indeed the absence of this peak, for the case of CNP-γ and WNP-γ, is interesting for potential application as starch matrices reinforcement. It should be noted that during production process aimed to develop biodegradable composites, the obtained nanoparticles will not suffer any thermal modification.

### 3.3. Mechanical characterization

SNP were employed as nanofiller in cassava starch matrix with the purpose to evaluate their applicability. It has been shown that

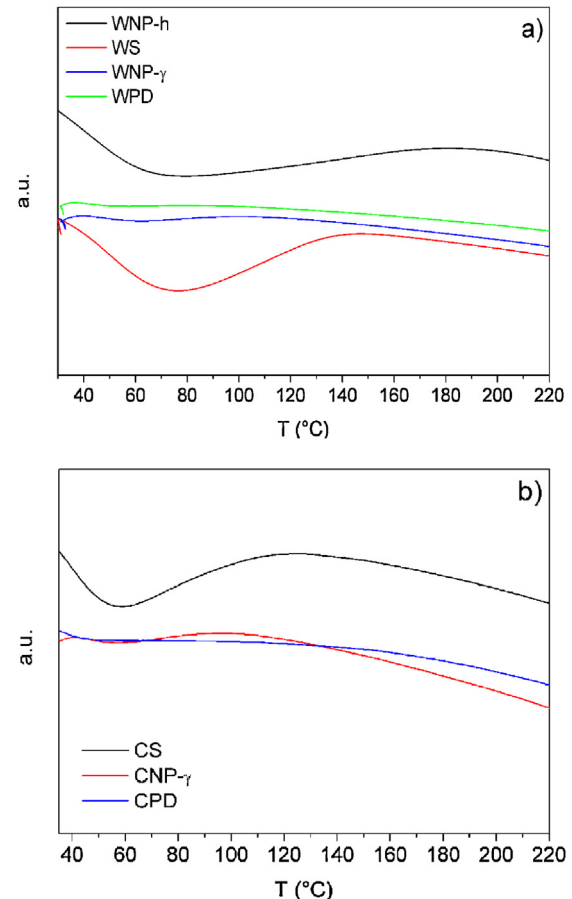


**Fig. 7.** DTA results obtained for waxy maize (a) and cassava (b) samples.

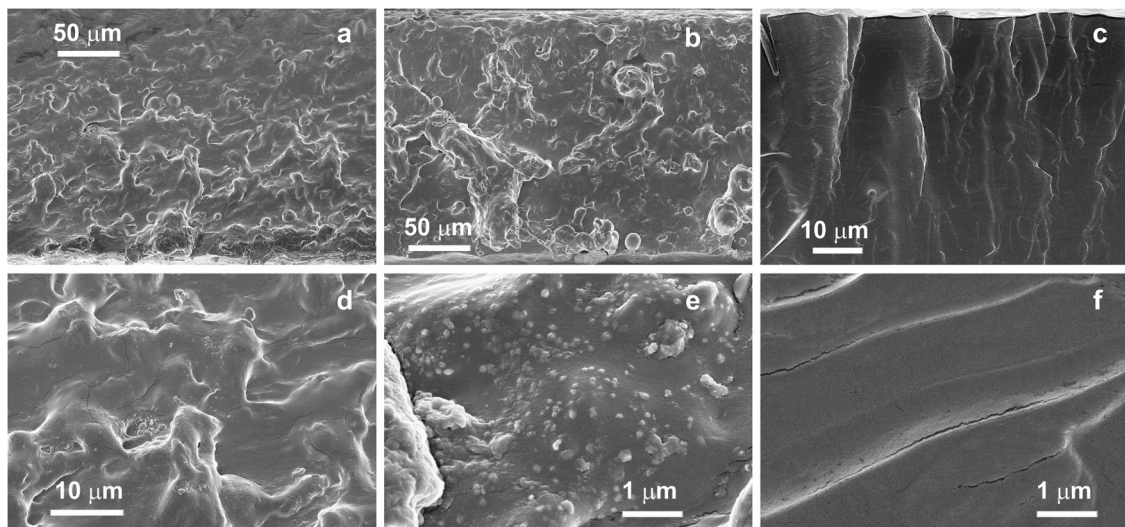


**Fig. 8.** FE-SEM micrographs for cryogenic fracture surface of: cassava matrix (a); cassava matrix with CNP- $\gamma$  (b), (d) and (e); cassava matrix with WNP- $\gamma$  (c) and (f).

the addition of nanoparticles obtained by acid hydrolysis technique (WNP-h) in cassava (García et al., 2009) or waxy maize (García et al., 2011) matrices led to storage modulus increments higher than 100%. WNP-h are crystalline and they acted as rigid reinforcement. The incorporation of 2.5% of CNP- $\gamma$  in the cassava matrix produced no significant changes in storage modulus while the addition of same amount of WNP- $\gamma$  led to increases of 102%. This difference can be explained taking into account the different dispersion of WNP- $\gamma$  and CNP- $\gamma$  in the matrix. It is well known that nanofillers act efficiently as matrices reinforcement but only if they are well dispersed, so interface with the matrix would be maximized (Famá, Pettarin, Goyanes, & Bernal, 2011).

In order to analyze the difference observed in mechanical properties, cryogenic fracture surfaces of plasticized starch films (matrix and matrix with CNP- $\gamma$  and WNP- $\gamma$ ) were studied (Fig. 8). In Fig. 8a is shown the surface of cassava matrix which was similar to that obtained for cassava matrix reinforced with CNP- $\gamma$  (Fig. 8b, d and e). On the contrary, for cassava matrix reinforced with WNP- $\gamma$  (Fig. 8c and f) it is possible to observe the typical veins pattern for a well dispersed SNP in starch matrix. A well developed vein pattern suggests that the deformation behavior is still controlled by the residual amorphous matrix (Bian, He, & Chen, 2002; Zilli et al., 2005). Several studies in starch composites with different types of nanofiller have been shown that an increase in the filler content led to a decrease in the space between veins (Anglès & Dufresne, 2000; Famá et al., 2011; Wilhelm, Sierakowski, Souza, & Wypych, 2003). A similar effect should occur when, for a given filler content, the distance between particles is decreased due to a better dispersion of the filler in the matrix. As a consequence of this effect, a composite with well dispersed NP should exhibit a more developed vein pattern. A similar result was reported by our research group for a cassava starch matrix and SNP obtained by acid hydrolysis treatment (García et al., 2009).

The addition of WNP- $\gamma$  in a cassava matrix had a lower storage modulus increase than the increment achieved with WNP-h (García et al., 2009). This difference could be explained taking into account that the crystallinity percent observed for WNP-h is much higher than the obtained for WNP- $\gamma$ . However, the use of these SNP is not limited to improve the mechanical properties; in fact they could also have another industrial application such as thickening agents. This is highly important since it is known that the addition of nanoparticles greatly increases the viscosity with an extremely low incorporation, as was reported by Kaya-Celiker and Mallikarjunan (2012).

Finally, it should be mentioned that although the nanoparticles obtained by acid hydrolysis (WNP-h) produced the highest increment in storage modulus, those obtained after gamma radiation (WNP- $\gamma$ ) also produced a significant improvement in terms of lower production costs, as purification treatments are not required, which greatly reduces the time and cost of SNP industrial production.

#### 4. Conclusions

Starch nanoparticles were obtained from waxy maize and cassava starches by gamma radiation of water starch dispersions. SNP average sizes determined by Dynamic Light Scattering were  $(31 \pm 5)$  nm and  $(41 \pm 7)$  nm for CNP- $\gamma$  and WNP- $\gamma$ , respectively.

The obtained nanoparticles of either type of starch had an amorphous XRD pattern. Amorphization was caused by the treatment necessary to obtain stable dispersions rather than by the gamma radiation. CNP- $\gamma$  and WNP- $\gamma$  showed the same thermal degradation behavior and the maximum weight loss zone was similar to those starch nanoparticles obtained from acid hydrolysis (WNP-h).

The addition of CNP- $\gamma$  as cassava matrix reinforcement did not significantly increase storage modulus. However, the use of WNP- $\gamma$  led to the development of starch nanocomposites with an enhancement in storage modulus of 102%.

Finally, it is possible to conclude that gamma radiation arises as an advantageous alternative to mass production of starch nanoparticles with low cost and using a simple and scalable methodology.

#### Acknowledgements

The authors are thankful for funds of Buenos Aires University (UBACYT No: 20020100100350) and CONICET PIP (Project 11220090100699).

#### Appendix A. Supplementary data

Supplementary data associated with this article can be found, in the online version, at <http://dx.doi.org/10.1016/j.carbpol.2013.04.081>.

## References

- Akhavan, A., & Ataeifarjovi, E. (2012). The effect of gamma irradiation and surfactants on the size distribution of nanoparticles based on soluble starch. *Radiation Physics and Chemistry*, 81, 913–914.
- Angellier, H., Molina-Boisseau, S., Dole, P., & Dufresne, A. (2006). Thermoplastic starch-waxy maize maize starch nanocrystals nanocomposites. *Biomacromolecules*, 7, 531–539.
- Angellier-Coussy, H., Putaux, J.-L., Molina-Boisseau, S., Dufresne, A., Bertoft, E., & Perez, S. (2009). The molecular structure of waxy maize starch nanocrystals. *Carbohydrate Research*, 344, 1558–1566.
- Anglès, M. N., & Dufresne, A. (2000). Plasticized starch/tunicin whiskers nanocomposites: 1. Structural analysis. *Macromolecules*, 33, 8344–8353.
- Bao, J., Ao, Z., & Jane, J. (2005). Characterization of physical properties of flour and starch obtained from gamma-irradiated white rice. *Starch/Stärke*, 57, 480–487.
- Bank, W., Greenwood, C. T., & Muir, D. D. (1973). The characterization of starch and its components. *Starch/Stärke*, 25, 405–408.
- Behera, A. K., Avancha, S., Sen, R., & Adhikari, B. (2013). Development and characterization of plasticized starch-based biocomposites with soy pulp as reinforcement filler. *Journal of Applied Polymer Science*, 127, 4681–4687.
- Bian, Z., He, C., & Chen, G. L. (2002). Investigation of shear bands under compressive testing for Zr-base bulk metallic glasses containing nanocrystals. *Scripta Materialia*, 46.
- Dufresne, A., & Cavaille, J. (1998). Clustering and percolation effects in microcrystalline starch-reinforced thermoplastic. *Journal of Polymer Science Part B: Polymer Physics*, 36, 2211–2224.
- Duquesne, E., Habibi, Y., & Dufresne, A. (2012). Novel nanocomposites reinforced with polysaccharide (starch) nanocrystals: From interfacial ring-opening polymerization to melt-processing implementation. In P. B. Smith, & R. A. Gross (Eds.), *Biobased monomers, polymers, and materials* (pp. 257–268). Washington, DC: American Chemical Society.
- Eid, M., Abdel-Ghaffar, M. A., & Dessouki, A. M. (2009). Effect of maleic acid content on the thermal stability, swelling behaviour and network structure of gelatin-based hydrogels prepared by gamma irradiation. *Nuclear Instruments and Methods in Physics Research Section B: Beam Interactions with Materials and Atoms*, 267, 91–98.
- El-Arnauty, M. B., Eid, M., Salah, M., & Hegazy, E. A. (2012). Preparation and characterization of poly vinyl alcohol/poly vinyl pyrrolidone/clay based nanocomposite by gamma irradiation preparation and characterization of poly vinyl alcohol/poly vinyl pyrrolidone/clay based nanocomposite by gamma irradiation. *Journal of Macromolecular Science Part A: Pure and Applied Chemistry*, 49, 1041–1051.
- Famá, L. M., Pettarin, V., Goyanes, S. N., & Bernal, C. R. (2011). Starch/multi-walled carbon nanotubes composites with improved mechanical properties. *Carbohydrate Polymers*, 83, 1226–1231.
- Garcia, V., Colonna, P., Bouchet, B., & Gallant, D. J. (1997). Structural changes of cassava starch granules after heating at intermediate water contents. *Starch/Stärke*, 49, 171–179.
- García Nancy, L., Ribba, L., Dufresne, A., Aranguren, M. I., & Goyanes, S. (2009). Physico-mechanical properties of biodegradable starch nanocomposites. *Macromolecular Materials and Engineering*, 294, 169–177.
- García, N. L., Ribba, L., Dufresne, A., Aranguren, M., & Goyanes, S. (2011). Effect of glycerol on the morphology of nanocomposites made from thermoplastic starch and starch nanocrystals. *Carbohydrate Polymers*, 84, 203–210.
- García, N. L., Lamanna, M., D'Accorso, N., Dufresne, A., Aranguren, M., & Goyanes, S. (2012). Biodegradable materials from grafting of modified PLA onto starch nanocrystals. *Polymer Degradation and Stability*, 97, 2021–2026.
- Guven, O. (2009). Controlling of degradation effects in radiation processing of polymer. In *IAEA TECDOC1617. Controlling molecular weights of polysaccharides*. Vienna: IAEA Publications.
- Hoover, R. (2000). Acid-treated starches. *Food Reviews International*, 16, 369–392.
- Jenkins, P. J., Comerson, R. E., Donald, A. M., Bras, W., Derbyshire, G. E., Mant, G. R., et al. (1994). In situ simultaneous small and wide angle X-ray scattering: A new technique to study starch gelatinization. *Journal of Polymer Science Part B: Polymer Physics*, 32, 1579–1583.
- Jolivet, J.-P., Livage, J., & Henry, M. (2000). Metal oxide chemistry and synthesis from solution to solid state. In J. W. Sons (Ed.), *Stability of colloidal dispersions* (pp. 256–283). New York: John Wiley.
- Kaya-Celiker, H., & Mallikarjunan, K. (2012). Better nutrients and therapeutics delivery in food through nanotechnology. *Food Engineering Reviews*, 4, 114–123.
- Labet, M., Thielemans, W., & Dufresne, A. (2007). Polymer grafting onto starch nanocrystals. *Biomacromolecules*, 8, 2916–2927.
- Le Corre, D., Bras, J., & Dufresne, A. (2010). Starch nanoparticles: A review. *Biomacromolecules*, 11, 1139–1153.
- Piyada, K., Waranyou, S., & Thawien, W. (2013). Mechanical, thermal and structural properties of rice starch films reinforced with rice starch nanocrystals. *International Food Research Journal*, 20, 439–449.
- Pimentel, T., Durães, J., Drummond, A., Schlemmer, D., Falcão, R., & Sales, M. (2007). Preparation and characterization of blends of recycled polystyrene with cassava starch. *Journal of Materials Science*, 42, 7530–7536.
- Singh, S., Singh, N., Ezekiel, R., & Kaur, A. (2011). Effects of gamma-irradiation on the morphological, structural, thermal and rheological properties of potato starches. *Carbohydrate Polymers*, 83, 1521–1528.
- Solinas, S., Piccaluga, G., Morales, M. P., & Serna, C. J. (2001). Sol-gel formation of  $\gamma\text{-Fe}_2\text{O}_3/\text{SiO}_2$  nanocomposites. *Acta Materialia*, 49, 2805–2811.
- Sreekumar, P., Al-Harthi, M. A., & De, S. (2012). Reinforcement of starch/polyvinyl alcohol blend using nano-titanium dioxide. *Journal of Composite Materials*, 46, 3181–3187.
- Vogel, A. (1983). *Química analítica cualitativa* (6th ed., pp.). Argentina: Kapelusz Eds.
- Wilhelm, H.-M., Sierakowski, M.-R., Souza, G. P., & Wypych, F. (2003). Starch films reinforced with mineral clay. *Carbohydrate Polymers*, 52, 101–110.
- Xu, Z., Sun, Y., Yang, Y., Ding, J., & Pang, J. (2007). Effect of  $\gamma$ -irradiation on some physicochemical properties of konjac glucomannan. *Carbohydrate Polymers*, 70, 444–450.
- Yu, Y., & Wang, J. (2007). Effect of  $\gamma$ -ray irradiation on starch granule structure and physicochemical properties of rice. *Food Research International*, 40, 297–303.
- Zilli, D., Chiliotte, C., Escobar, M. M., Bekeris, V., Rubiolo, G. R., Cukierman, A. L., et al. (2005). Magnetic properties of multi-walled carbon nanotube-epoxy composites. *Polymer*, 46, 6090–6095.